

LINEAR POLARIZATION AND SPECTRUM OF PSR 0833—45 AND THE EFFECTS OF SCATTERING

By M. M. KOMESAROFF,* P. A. HAMILTON,† and J. G. ABLES*

[Manuscript received 13 July 1972]

Abstract

Linear polarization characteristics as well as pulse shape have been measured at Parkes for the average of many pulses from PSR 0833—45 at several frequencies between 300 and 1410 MHz. These confirm a previous conclusion, which was based on pulse shape measurements alone, that the change of pulse character with decreasing frequency can be explained in terms of interstellar scattering. The inferred effect of the scattering medium is explained on the assumption that it comprises many layers of weak uncorrelated density inhomogeneities. Also, some evidence is found for a weak “precursor” pulse, and the possible implications are discussed.

I. INTRODUCTION

In order to provide constraints that must be met by any acceptable theory of the pulsar phenomenon, it is clearly desirable to measure pulse characteristics over as wide a frequency range as possible. Such measurements also provide information about the structure of the interstellar medium. The pulsar PSR 0833—45 is a very suitable subject for this type of measurement because its pulse intensity remains steady over long periods of time. This makes it possible to determine the average pulse shape and linear polarization characteristics at a number of frequencies simultaneously, by using a single linearly polarized feed at each frequency. Radhakrishnan *et al.* (1969) and Radhakrishnan and Cooke (1969) first showed that the sweep of polarization position angle through the pulse is large and invariant over a range of frequencies above 1400 MHz, a result which essentially established the rotating neutron star model of the pulsar.

Here we report measurements made at Parkes at a number of frequencies between 300 and 1410 MHz. These show that the frequency-invariance of intrinsic position angle persists to the lower frequencies. This enables us to draw certain conclusions about the radiation mechanism.

The observational results are reported in detail in Section III. The additional information provided by the present polarization measurements substantiates the earlier conclusion of Ables, Komesaroff, and Hamilton (1970) that the marked pulse-broadening observed at low frequencies is due to interstellar scattering. The broadening is found to be accompanied by changes in both the degree of linear polarization

* Division of Radiophysics, CSIRO, P.O. Box 76, Epping, N.S.W. 2121.

† Department of Physics, University of Tasmania, Hobart, Tas. 7001.

and in the rate of change of polarization position angle through the pulse. It is found that the low-frequency pulse characteristics can be derived with some accuracy by convolving each time-dependent Stokes parameter of the observed 1410 MHz pulse with a truncated exponential function, the scale of which varies as ν^{-4} , where ν is the frequency.

This result is consistent with scattering from a localized region of the interstellar medium that produces a Gaussian "angular spectrum" of scattered radiation. Previous authors (Fejer 1953; Bramley 1954) have discussed scattering from an irregular medium and have derived an approximately Gaussian angular spectrum. However, their derivations rest on the special assumption that the spatial autocorrelation function of density irregularities is also Gaussian. In Section IV it is shown that this assumption is unnecessary and that, under fairly general conditions, a medium comprising many layers of weak uncorrelated density fluctuations would produce a Gaussian angular spectrum of scattered radiation.

The observations also suggest that there may be a "precursor" to PSR 0833-45, in some ways analogous to that observed in the case of NP 0532. It is argued that this could be produced by a scattering medium associated with the pulsar itself.

In Section V the observed interstellar scattering effects are discussed in relation to independent data for the Gum nebula, in which the pulsar is believed to be immersed. Finally, in Section VI the present results and those of other observers are discussed in terms of current theories of pulsar emission.

II. OBSERVATIONS

(a) *Method*

Basically, the technique was that described by Ables, Komesaroff, and Hamilton (1970). Four receivers tuned to frequencies near 300, 400, 630, and 1410 MHz were operated simultaneously. Each receiver had its own linearly polarized feed. The detected receiver outputs were fed through a rapid multiplexer to a PDP-9 computer, which also received a time-base signal at the Doppler-shifted pulsar period. For a fixed feed position angle, the intensity at each frequency, averaged over several thousand pulses, was computed at intervals of 1/200 of a period by the method of superposed epoch analysis. After each average had been formed, the whole feed assembly was rotated in position angle and the process repeated. Measurements were made over the range of feed position angles between $+90^\circ$ and -90° at intervals of 30° or less, with some repetitions to provide a consistency check. The procedure occupied two to three hours on each observing day.

The data were recorded on punched tape and subsequently computer-analysed to yield the total intensity, linearly polarized intensity, and position angle of the linear polarization, each sampled at intervals of 1/200 of a period. One such set of average profiles was derived for each observing frequency and for each day. In carrying out the reductions certain corrections were made to the data:

- (1) The effects of slow variations of receiver gain and pulse intensity were corrected. To make this possible the original measurements were taken in pairs, one position angle being immediately followed by the position angle orthogonal to it. The sum of such a pair of averages constituted the "total intensity" pulse,

and ideally all such sums should have been the same. Where they were not, normalizing factors were applied to equalize the peak intensities.

- (2) Corrections were applied for the small difference between the periods of the pulsar and the time base, which manifested itself as a slow drift of the pulse peak with time.
- (3) The average ionospheric Faraday rotation for each frequency during each integration was calculated from values of $f_0 F_2$ published by the Australian Ionospheric Prediction Service, by means of a computer program kindly made available by Dr. J. B. Whiteoak. From this, the "effective" position angle of each feed, as referred to a point above the ionosphere, was calculated.

(b) Receivers

The observations were made on 8 and 9 May 1970. The centre frequencies ν and bandwidths $\Delta\nu$ used were:

8 May 1970

ν (MHz)	1409.8	628.4	468.04	466.56	410.16	408.68	299.21
$\Delta\nu$ (MHz)	1.0	0.1	0.1	0.1	0.1	0.1	0.1

9 May 1970

ν (MHz)	1410.47	629.09	467.74	409.01	301.17	297.17
$\Delta\nu$ (MHz)	1.0	1.0	0.1	0.1	0.1	0.1

For all receivers the time constant was 0.47 ms, approximately equal to the sampling interval.

The "400 MHz" receiver was operated in the double-sideband mode, so that with one 30 MHz i.f. channel it accepted a range of frequencies 100 kHz wide centred near 408 MHz and another range of equal width centred near 468 MHz. Dispersion delay ensured that the pulse arrival times at the two frequencies were such that there was no pulse overlap. On 8 May 1970, the 400 MHz receiver was used in conjunction with the back-end of a multichannel line receiver. The outputs of two channels, equivalent to two independent i.f. systems, were recorded. Thus on that day four separate records were obtained from the 400 MHz receiver, two at slightly separated frequencies near 408 MHz and two near 468 MHz. All other receivers were operated in the single-sideband mode. On 9 May, the 300 MHz receiver was used with the multichannel back-end.

(c) Calibration

The centre frequencies of all receiver channels were measured at intervals throughout the observing session by lightly coupling a signal from a tunable oscillator into the feed system. The oscillator frequency was measured with a Hewlett-Packard frequency counter.

Intensity calibrations were derived from a 10^4 K argon noise lamp fed to a doubly-balanced ring modulator. The modulator output was split in a passive network so as to provide one calibrating signal for each receiver. A signal from the PDP-9 computer controlled the modulator so that the calibrating signal was applied for a very short fraction of each pulsar period, at a phase of the cycle when the radiation was negligibly weak at all observing frequencies.

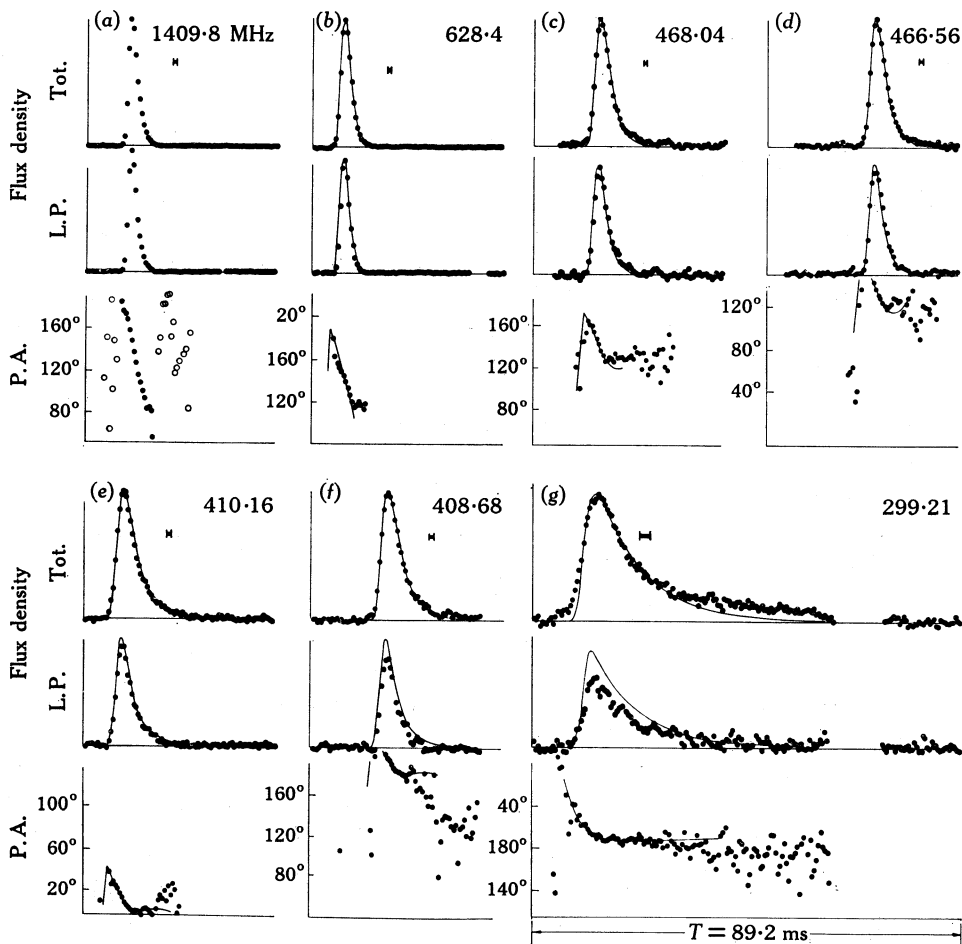
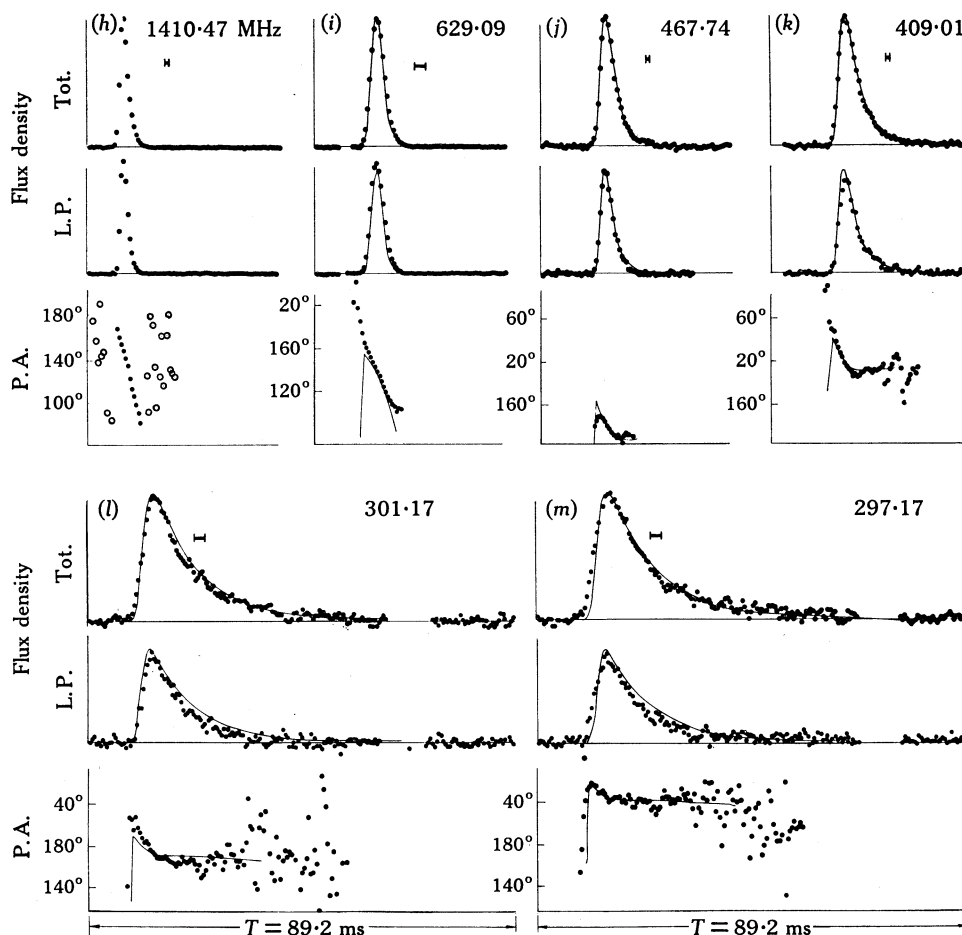


Fig. 1.—Average values of total intensity, linearly polarized intensity (L.P.), and polarization position angle (P.A.) of pulsar PSR 0833—45, for the indicated frequencies, as measured on: (a)–(g) 8 May 1970 and (h)–(m) 9 May 1970. The filled circles indicate observed values and the continuous curves represent values obtained by convolution of the corresponding 1410 MHz data with $f(t, \tau)$ as indicated in the text. The time scale is the same in all cases and 89.2 ms is the period between pulses. The short horizontal bars show the extent of “dispersion smearing” by the finite receiver bandwidth. The open circles in (a) and (h) indicate position angles corresponding to low values of flux density.

III. OBSERVATIONAL RESULTS

(a) Comparison of Observed and Computed Pulse Characteristics

Figures 1(a)–1(m) show the results of our observations for each frequency on the two observing days (some of the data appearing in Figs. 1(a)–1(g) have been presented previously by Komesaroff, Hamilton, and Ables 1971). The average measured values of total flux density, linearly polarized flux density, and polarization position angle are indicated by filled circles (at 1410 MHz, position angles corresponding to very low values of flux density are indicated by open circles). The flux density scales for the various frequencies are arbitrary, but for any one frequency the same scale has



Figs. 1(h)–1(m).

been used for the total and the linearly polarized flux density, so that the degree of linear polarization is unchanged.

The very marked increase of pulse duration at the lower frequencies, as shown in these figures, was first observed by Ables, Komesaroff, and Hamilton (1970) and attributed by them to interstellar scattering. The present results show that the pulse broadening is accompanied by a decrease in the degree of linear polarization at the pulse peak and also a decrease in the rate of change of polarization position angle through the pulse. We will see that interstellar scattering can account for these effects.

To demonstrate this we need a model of the unscattered pulse. The observations of Radhakrishnan and Cooke (1969) show that there is little variation in the characteristics of the pulses from PSR 0833-45 between 1410 and 1720 MHz. Accordingly we conclude that the intrinsic pulse characteristics are the same at these widely spaced frequencies and that scattering has negligible effect at frequencies of 1410 MHz and higher. For the moment we will assume that the intrinsic pulse characteristics remain substantially invariant as the observing frequency decreases below 1410 MHz.

In Section IV it is shown that under certain conditions the effect of interstellar scattering may be approximated by convolving each of the time-dependent Stokes parameters of the unscattered pulse with a truncated exponential function of the form

$$\left. \begin{aligned} f(t, \tau) &= \tau^{-1} \exp(-t/\tau) & \text{for } t \geq 0, \\ &= 0 & t < 0. \end{aligned} \right\} \quad (1)$$

where τ is proportional to ν^{-4} , ν being the frequency. We refer to $f(t, \tau)$ as the "impulse response function" of the medium.

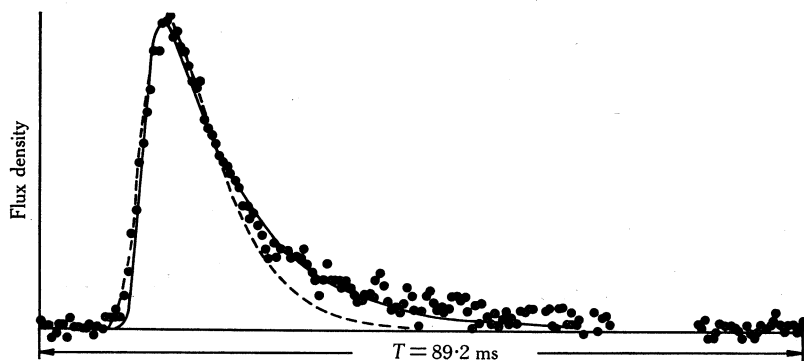


Fig. 2.—Comparison between the average observed 297.17 MHz pulse (filled circles) for 9 May 1970 and the pulse shapes derived by convolving the average observed 1410.47 MHz pulse for the same day with the functions $f(t, \tau)$ (continuous curve) and $g(t, \tau')$ (dashed curve) defined in the text. The values of τ and τ' were chosen to give the best fit at the pulse peak.

The effect of scattering is most marked at the lowest observing frequency (300 MHz). We have accordingly estimated the "scattering time" at 300 MHz, $\tau(300)$, by convolving the total-intensity pulse observed at 1410 MHz with the truncated exponential $f(t, \tau)$, given by the form (1), for various values of τ until the best fit was obtained to the 300 MHz pulse shape. The result is shown in Figure 2, in which the filled circles represent the observed flux density at 297.17 MHz as measured on 9 May 1970 and the full line represents the result of the convolution for $\tau(300) = 9.4$ ms.* The observed and computed pulse shapes agree well, particularly on the trailing edge of the pulse.

Now, in the case of the pulsar NP 0532, which also shows the effects of marked scattering at low frequencies, Rankin *et al.* (1970) have found that the observed low-frequency pulse shape can best be approximated by convolving the high-frequency pulse, not with a truncated exponential $f(t, \tau)$ such as we have used, but rather with a function of the form $g(t, \tau')$, where

$$\left. \begin{aligned} g(t, \tau') &= (t/\tau'^2) \exp(-t/\tau') & \text{for } t \geq 0, \\ &= 0 & t < 0. \end{aligned} \right\}$$

* Both here and for all convolution results presented later, additional "smoothing" to simulate the effect of the known dispersion delay within the finite receiver pass band has also been performed.

We have tried the effect of convolving the high-frequency pulse from PSR 0833-45 with $g(t, \tau')$, choosing that value of τ' which gives the best fit near the observed pulse peak. The result is indicated by the dashed line in Figure 2. It is clear that the truncated exponential $f(t, \tau)$ gives a considerably better fit. A similar procedure carried out using other measurements near 300 MHz for both 8 and 9 May gave the same result. Accordingly, for both days we have convolved the 1410 MHz data with $f(t, \tau)$ in an attempt to reproduce the pulse shapes and polarizations at all observing frequencies. For a frequency ν MHz the value of τ used was given by

$$\tau(\nu) = (300/\nu)^4 \tau(300),$$

where $\tau(300) = 9.4$ ms, as indicated above.

The results of the convolutions are indicated in Figures 1(a)–1(m) by the continuous curves. The only adjustments made to the computed data in drawing the curves were as follows.

- (1) The flux density scales were normalized so that the peak value of total flux density (or first Stokes parameter) agreed with the observed value. This left the computed instantaneous degree of polarization unaltered.
- (2) The figures were shifted horizontally so that the peak of the computed total intensity pulse was aligned with the observed peak. This adjustment was necessitated by the ν^{-2} interstellar dispersion delay.
- (3) The position angle scale was shifted vertically so that the computed position angle at the pulse peak was brought into agreement with the observed value. This shift compensated for interstellar Faraday rotation.

Interstellar dispersion and Faraday rotation are considered in more detail below.

Apart from some discrepancies discussed in subsection (c) below, there is good agreement, at all the observing frequencies, between the observed and computed values for both pulse shapes and linear polarization characteristics. The results therefore support the conclusion reached by Ables, Komesaroff, and Hamilton (1970) that the increase of pulse duration with decreasing frequency is due to interstellar scattering, and they also support the present assumption that the intrinsic pulse characteristics are substantially frequency-invariant below 1410 MHz.

The convolution results indicated the amount by which the arrival time of the pulse peak and the position angle at the peak were modified by scattering alone. After correction was made for these effects, the arrival time T of the peak showed a precise linear dependence on λ^2 (where λ is the wavelength), with a slope corresponding to

$$dT/d(\lambda^2) = 3.18863 \pm 0.0003 \text{ s m}^{-2},$$

or a dispersion measure of $69.08 \pm 0.01 \text{ cm}^{-3} \text{ pc}$, which is in accordance with previous estimates. The r.m.s. scatter of points about the line of best fit was ~ 0.3 ms. A similar procedure for the position angle θ yielded a rotation measure

$$d\theta/d(\lambda^2) = 33.6 \pm 0.1 \text{ rad m}^{-2}$$

and a polarization position angle at the peak of the pulse extrapolated to zero wavelength (subsequently referred to as the "intrinsic" position angle) of $63^\circ.1 \pm 1^\circ.5$.

The r.m.s. scatter about the line of best fit was $\sim 4^\circ$. Any systematic departures from the linear relationship did not exceed the measuring errors in either case. Independent estimates for the data of each observing day agreed within the quoted uncertainties.

The rotation and dispersion measures together yield a weighted mean longitudinal magnetic field strength of $0.6 \mu\text{G}$, which is of the same order as other estimates of the galactic magnetic field. Thus the present results are consistent with the view that, before being modified by interstellar scattering and Faraday rotation, the instantaneous degree and position angle of the polarization are substantially frequency-invariant from 300 to 1400 MHz. There is therefore no evidence of any substantial Faraday rotation associated with the pulsar magnetosphere.

The rotation measure and intrinsic position angle quoted above are in good agreement with the values of $33 \pm 6 \text{ rad m}^{-2}$ and $57^\circ \pm 6^\circ$ respectively, which were derived by Ekers *et al.* (1969) from measurements made more than a year before those reported here. Ekers *et al.* based their estimates on measurements at 1430, 1700, and 2300 MHz, representing a range of about 0.027 m^2 in λ^2 . The corresponding range for the present measurements is 0.96 m^2 , which is greater by a factor of more than 30, and thus our estimated errors are very much smaller than theirs.

On the other hand, there is a significant discrepancy between the present results and those of Radhakrishnan and Cooke (1969). Their measurements at 1420, 1720, and 2700 MHz yielded a rotation measure of $42 \pm 4 \text{ rad m}^{-2}$ and an intrinsic position angle of 47° . The probable reason for the discrepancy is indicated by the following comparison of values for the polarization position angle at pulse peak.

ν (MHz)	1420	1720	2700	∞
Present results	$149^\circ \pm 1^\circ.8$	$[122^\circ \pm 1^\circ.7]$	$[87^\circ \pm 1^\circ.5]$	$[63^\circ.1 \pm 1^\circ.5]$
Radhakrishnan and Cooke (1969)	$154^\circ \pm 5^\circ$	$120^\circ \pm 5^\circ$	$76^\circ \pm 8^\circ$	$[\sim 47^\circ]$

Here our best estimate of the position angle at 1420 MHz is given together with values extrapolated from our data to 1720 and 2700 MHz (all extrapolated results are enclosed by square brackets). The position angles quoted for Radhakrishnan and Cooke are taken from their Table I (1420 and 1720 MHz) and Figure 1 (2700 MHz). A comparison of intrinsic position angles is also made. At 1420 and 1720 MHz the results agree within the experimental errors. Only at 2700 MHz does the discrepancy between the two sets of results slightly exceed the sum of the quoted experimental uncertainties. However, as mentioned by Radhakrishnan and Cooke, the 500 MHz effective bandwidth which they used at 2700 MHz would produce significant dispersion broadening (about 14 ms, or some seven times the intrinsic half-power pulse width as measured at the lower frequencies). Therefore the two sets of data can be reconciled on the assumption that Radhakrishnan and Cooke slightly underestimated their measuring error at 2700 MHz, a substantial part of which was due to dispersion broadening.

Thus there is no evidence for a change in either intrinsic position angle or rotation measure during the interval of more than one year that elapsed between the earlier measurements and ours. Furthermore, when taken together, the results substantiate the conclusion of Radhakrishnan and Cooke (1969) that the jump in pulsar period

which occurred between two sets of observations made by them was not accompanied by any change in the pulsar magnetic field structure.

(b) *Initial Positive Sweep of Position Angle*

Figures 1(a)–1(m) illustrate a feature first observed by McCulloch *et al.* (1972), namely, a rapid increase in polarization position angle near the time of pulse onset. This is particularly noticeable in Figures 1(c), 1(d), and 1(m) and is followed by the well-known decrease in position angle through the major part of the pulse. McCulloch *et al.* observed the effect at 400 MHz.

The present results provide some evidence that the effect may be present at frequencies as high as 1410 MHz. This is shown by the fact that the initial positive swing appears in the *predicted* position angle curves at almost all the lower frequencies (Figs. 1(a)–1(m)). Since the predicted curves are derived from the observed 1410 MHz data by the convolution process described in subsection (a), and since it can be shown that the initial sense of rotation of position angle is unaffected by the convolution, it follows that a sudden change of polarization must be present in the 1410 MHz observational data. Although this is not evident in the plotted points, the smoothing process of convolution reveals a sudden change. High sensitivity 1410 MHz observations would be of interest in this regard.

However, the results of McCulloch *et al.* (1972) leave no doubt about the reality of the effect at 400 MHz. These authors suggest that it may be associated with a phenomenon analogous to the precursor which precedes the main pulse of NP 0532 and which has been observed at only the lower radio frequencies (Campbell, Heiles, and Rankin 1970; Rankin *et al.* 1970; Rankin, Heiles, and Comella 1971). The present results provide some support for this view, since they show a weak enhancement of flux density preceding the main pulse. The enhancement is most clearly marked at our lowest observing frequencies: 299.21 MHz on 8 May (Fig. 1(g)) and 297.17 MHz on 9 May (Fig. 1(m)). It occurs from about 1/20 to 1/10 of a period before the main pulse peak. In the case of NP 0532 the precursor occurs 1/20 of a period before the main peak.

Finally, Figure 1(g) shows that the trailing edge of the 299.21 MHz pulse on 8 May decays more slowly than the simple interstellar scattering theory would predict, and the same figure shows the initial flux density enhancement most clearly. Near the same frequency on 9 May (Figs. 1(l) and 1(m)) the trailing edge of the pulse shows good agreement with prediction. This change over a period of one day suggests an effect associated with the pulsar itself rather than with the interstellar medium. Komesaroff (1971) has argued that, in the case of NP 0532, the precursor could result from scattering in a medium surrounding the pulsar at a distance approximately equal to the velocity-of-light radius. The foregoing results suggest that PSR 0833-45 may be surrounded by a similar medium and that its density fluctuates in a time interval of about one day.

(c) *Rise Time of Low-frequency Pulse*

There is a small but significant discrepancy between the predicted and observed shape of the leading edge of the pulse. In general the predicted rise time is more rapid than that actually observed (see in particular Figs. 1(g), 1(l), and 1(m)). This may

indicate intrinsic pulse broadening at the lower frequencies. On the other hand, it may indicate the inadequacy of the simple truncated exponential approximation to the true impulse response function of the medium. Whatever the explanation, we obtain a better fit to the observed 300 MHz data if, after first convolving the observed 1410 MHz pulse with $f(t, \tau_1)$, we then further convolve it with $f(t, \tau_2)$, where

$$\tau_1(300) = 9.4 \text{ ms} \quad \text{and} \quad \tau_2(300) = 0.9 \text{ ms}.$$

(d) *Low-frequency Spectral Turnover*

Figure 3 shows our measured values of average flux density and also the 80 MHz measurement of Higgins, Komesaroff, and Slee (1971), who employed a technique which did not distinguish between the pulsed component and any steady component of flux density. Although there is some scatter, due presumably to calibration errors, Figure 3 indicates that the flux density down to 80 MHz is approximately proportional to $\nu^{-\alpha}$, with $\alpha = 0.9$.

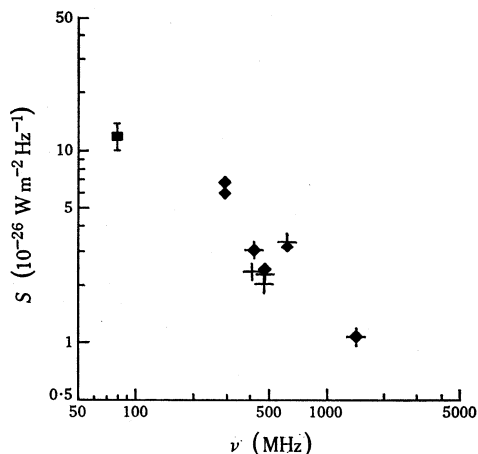


Fig. 3.—Flux density S , averaged over one pulse period, as a function of frequency ν . The present observations of pulsed flux density on 8 May and 9 May 1970 are represented by crosses and diamonds respectively. The square represents the total flux density measurement by Higgins, Komesaroff, and Slee (1971) made with the 80 MHz Culgoora heliograph during May 1971. The 299.21 MHz observation for 8 May 1970 has been omitted as there was evidence of a large calibration error on that day.

From the figure, the predicted flux density at 150 MHz would be approximately $7 \times 10^{-26} \text{ W m}^{-2} \text{ Hz}^{-1}$ or $0.6 \times 10^{-26} \text{ J m}^{-2} \text{ Hz}^{-1}$ per pulse period. However, Ables, Komesaroff, and Hamilton (1970) set an upper limit on the 150 MHz pulse energy of $\sim 0.03 \times 10^{-26} \text{ J m}^{-2} \text{ Hz}^{-1}$, which is only about 0.05 of the above value. (Because of a computational error, the values of pulse energy quoted by Ables, Komesaroff, and Hamilton must be divided by two to obtain the correct values.)

Now, the scattering time τ , derived from the high-frequency measurements and extrapolated to 150 MHz, yields a value $\tau(150) \approx 150 \text{ ms}$, which is 1.7 times greater than the period between pulses (89.2 ms). This means that at 150 MHz there will be considerable overlap between successive pulses, with a consequent conversion of part of the emission into steady flux (which would not have been detected by Ables, Komesaroff, and Hamilton 1970). The effect is discussed quantitatively in Section IV(d) below; from equation (16) it can be shown that only about 0.2 of the emission will appear as pulsed flux. However, this is still very much larger than the upper limit set by Ables, Komesaroff, and Hamilton.

On the basis of the double convolution discussed in subsection (c) above, we predict a somewhat smaller residual pulsed flux density at 150 MHz, but one which is nevertheless larger than the upper limit set by Ables, Komesaroff, and Hamilton (1970). If the shape of the impulse response function is independent of frequency and only its scale varies as ν^{-4} then both τ_1 and τ_2 must vary as ν^{-4} , thereby yielding $\tau_1(150) \approx 150$ ms and $\tau_2(150) \approx 15$ ms. In that case the pulsed component of flux density is reduced to about 0.15 of the total.

Thus although a spectral turnover in the pulsed component of emission is to be expected, the results of Ables, Komesaroff, and Hamilton (1970) indicate that it is considerably sharper than we would predict. The above arguments indicate that we can explain the effect in terms of scattering only by assuming that below 300 MHz the scattering time is proportional to $\nu^{-\beta}$, where β is > 4 , contrary to the result derived in Section IV below.

The discussion in Section IV, which yields the result that $\beta = 4$, is based on the assumption that the scattering medium extends over only a small fraction of the distance between the pulsar and the Earth and is situated at a great distance from both. A more general discussion could possibly yield a different value of β .

If a substantial fraction of the scattering below 300 MHz occurs very close to the pulsar itself, several of the assumptions made in Section IV(a) below would not necessarily be valid. For example, if the fraction of the incident radiation scattered by the medium associated with the pulsar were small above 300 MHz and became large near 150 MHz, and if the scattering angle were also large, this component of the scattering would become dominant at low frequencies, contrary to one of our assumptions. Furthermore, if the scattering occurred close to the velocity-of-light cylinder the geometry involved would be entirely different from that assumed in Section IV and the results derived there would no longer apply.

IV. SCATTERING DUE TO AN INHOMOGENEOUS MEDIUM

(a) *Angular Spectrum*

The foregoing discussion has shown that, at least down to 300 MHz, the variation of pulse characteristics with frequency is consistent with scattering from a medium for which the impulse response function is approximately a truncated exponential that scales as ν^{-4} . Several authors (e.g. Cronyn 1970) have shown that the truncated exponential function finds a natural explanation in terms of scattering from a localized part of the interstellar medium, the scattering function being such that an incident plane wave is converted into a circular Gaussian angular distribution of radiation. Here we show that scattering would produce a Gaussian distribution in certain fairly general circumstances but not necessarily in all cases.

Consider a plane wave initially propagating in the z direction and impinging on a medium, the refractive index of which is spatially inhomogeneous. The medium is assumed to be widely extended in the x and y directions. After the wave has emerged from the medium it may be represented by the \mathbf{E} -vector distribution over a plane parallel to the xy plane. For a wave of angular frequency ω and a fixed direction of polarization we write this as $E(x, y) \exp(i\omega t)$, a complex function of the coordinates x and y . It will be convenient to measure x and y in terms of the free space wavelength. The effect of the medium on the wave may be characterized

by the two-dimensional autocorrelation function of the emergent field,

$$\rho(\xi, \eta) = \frac{\int_{-\infty}^{+\infty} \int_{-\infty}^{+\infty} E(x, y) E^*(x + \xi, y + \eta) dx dy}{\int_{-\infty}^{+\infty} \int_{-\infty}^{+\infty} E(x, y) E^*(x, y) dx dy}.$$

The emergent radiation can also be represented by its "angular power spectrum". If we restrict our analysis to small angles in the subsequent discussion, this may be written $F(\theta_x, \theta_y)$, where $F(\theta_x, \theta_y) d\theta_x d\theta_y$ is the component of power scattered into the solid angle $d\theta_x d\theta_y$ in the direction (θ_x, θ_y) . Here θ_x and θ_y are the angles between the direction of the wave component and the yz and xz planes respectively. The relation between $F(\theta_x, \theta_y)$ and $\rho(\xi, \eta)$ is the two-dimensional Fourier transform (see e.g. Ratcliffe 1956)

$$F(\theta_x, \theta_y) = \int_{-\infty}^{+\infty} \int_{-\infty}^{+\infty} \rho(\xi, \eta) \exp\{-2\pi i(\theta_x \xi + \theta_y \eta)\} d\xi d\eta. \quad (2)$$

If $F(\theta_x, \theta_y)$ is to be a Gaussian function, $\rho(\xi, \eta)$ must also be Gaussian. Hewish (1951) considered the general case of a random phase-changing medium and concluded that the autocorrelation function would indeed be approximately Gaussian when the r.m.s. phase deviation produced by the medium was small. However, he also showed that, as the phase deviation becomes greater than 1 rad, the Gaussian approximation becomes progressively less accurate.

The present observations indicate that the phase deviation is many radians at our observing frequencies (see Section IV(c)). Fejer (1953), on the basis of a model of more restricted generality than that of Hewish (1951), showed that even for the case of a very large phase deviation the angular spectrum produced by scattering would be approximately Gaussian. Bramley (1954) derived an identical result by a much simpler argument. However, both authors introduced one special *a priori* assumption which appears to be crucial, namely that the spatial autocorrelation function of the density irregularities in the medium is itself Gaussian. Here we show that this special assumption is not essential and that a large r.m.s. phase deviation can be reconciled with a Gaussian angular spectrum on the basis of a more general model of the interstellar medium.

We imagine the medium to be divided into a large number of scattering "screens" by planes perpendicular to the original direction of propagation (the z axis). We then make the assumptions that:

- (1) each screen is "thin", i.e. it modifies the phase but not the amplitude of the E -vector distribution of the radiation incident on it;
- (2) the phase fluctuations imposed by any one screen are not correlated with those imposed by any of the others;
- (3) for each screen the phase variations are random functions of the coordinates x and y and there are no large-scale phase gradients extending over many irregularities;
- (4) the r.m.s. phase change due to any one screen is $> 2\pi$ rad;

- (5) the phase fluctuations due to the medium as a whole are not dominated by those due to any one screen;
- (6) the linear scales of the irregularities producing the fluctuations are very much greater than the observing wavelength; and
- (7) magnetic fields in the scattering medium may be neglected.

For simplicity we first calculate the one-dimensional autocorrelation function $\rho(\xi) = \rho(\xi, 0)$ due to such a medium. For convenience of notation we shall omit the constant factor $\exp(i\omega t)$ in the complex amplitude. The distribution of complex amplitude which would be imposed on a plane wave of unit amplitude by the k th screen acting alone is denoted by $E_k(x)$ and the corresponding autocorrelation function is denoted by $\rho_k(\xi)$.

After the wave has traversed the first two screens, the complex amplitude distribution will be

$$E_1(x) E_2(x).$$

According to assumption (2) above $E_1(x)$ and $E_2(x)$ are uncorrelated. It therefore follows that the autocorrelation function $\rho_{1,2}(\xi)$ of the wave after it has traversed the first two screens is given by (see e.g. Papoulis 1965)

$$\rho_{1,2}(\xi) = \rho_1(\xi) \rho_2(\xi).$$

This result is independent of the spacing between the screens, because the amplitude autocorrelation function produced by any scattering screen does not change with distance along the z direction from the screen (Ratcliffe 1956).

By iteration it therefore follows that, after the wave has traversed the whole medium, the autocorrelation function is

$$\rho(\xi) = \rho_1(\xi) \rho_2(\xi) \dots \rho_k(\xi) \dots \rho_n(\xi).$$

The one-dimensional angular power spectrum $F(\theta_x)$ is given by

$$F(\theta_x) = \int_{-\infty}^{+\infty} \rho(\xi) \exp(-i2\pi\xi\theta_x) d\xi, \quad (3)$$

and therefore according to the convolution theorem

$$F(\theta_x) = f_1(\theta_x) * f_2(\theta_x) * \dots * f_k(\theta_x) * \dots * f_n(\theta_x), \quad (4)$$

where the asterisk denotes the convolution operation and

$$f_k(\theta_x) = \int_{-\infty}^{+\infty} \rho_k(\xi) \exp(-i2\pi\xi\theta_x) d\xi. \quad (5)$$

From assumption (3) above, it follows that $\rho_k(\xi)$ is a real function (Hewish 1951) and therefore from its definition is an even function having its maximum value at $\xi = 0$. Furthermore, as ξ increases from zero to a value ξ_0 , $\rho_k(\xi)$ becomes small and, for much larger values of ξ , approaches zero. Since ξ is expressed in units of the observing wavelength λ , and since the r.m.s. phase deviation $\delta\phi_k$ is

> 1 rad (assumption (4)), it follows that

$$\xi_0 \approx a_k/\lambda \delta\phi_k,$$

a_k being the linear "scale size" of one irregularity (see e.g. Ratcliffe 1956).

Now $f_k(\theta_x)$ is the angular power spectrum which would be produced by the k th screen acting alone. It is therefore positive (or zero) for all θ_x . From equation (3) and what has been said of $\rho_k(\xi)$, it follows that each $f_k(\theta_x)$ is an even function having its maximum values close to $\theta_x = 0$ and decreasing to a small value for

$$\theta_x \approx 1/2\pi\xi_0 = \lambda \delta\phi_k/2\pi a_k.$$

For very much larger values of θ_x , $f_k(\theta_x)$ approaches zero. Therefore, according to the central limit theorem, the repeated convolution represented by equation (4) yields a very good approximation to a Gaussian function for even relatively small values of n . The central limit theorem also indicates that for the medium as a whole θ_0 , the mean square value of θ_x , is given approximately by

$$\theta_0^2 \approx \sum_{k=1}^n (\lambda \delta\phi_k/2\pi a_k)^2. \quad (6)$$

If the medium is statistically homogeneous this may be written

$$\theta_0^2 \approx (\lambda\phi/2\pi a)^2 \quad (7)$$

$$= \left(\frac{r_0}{2\pi}\right)^2 \frac{L(\Delta N)^2}{a} \left(\frac{c}{\nu}\right)^4, \quad (8)$$

where r_0 is the classical electron radius (2.8×10^{-13} cm), L the thickness of the medium, ΔN the electron density fluctuation associated with one irregularity, c the velocity of light, ν the observing frequency, and ϕ the r.m.s. phase change due to the whole medium. Equation (7), giving the scattering angle, was derived by Scheuer (1968), using a slightly different approach. We have used his argument to derive equation (8) from (7).

The foregoing has shown that, under the conditions specified, the Fourier transform of $\rho(\xi, 0)$ is Gaussian. For a statistically homogeneous medium the two-dimensional autocorrelation function $\rho(\xi, \eta)$ is a function of r only (where $r^2 = \xi^2 + \eta^2$) and has the same form as $\rho(\xi, 0)$. It follows then that the angular power spectrum, the two-dimensional Fourier transform of $\rho(\xi, \eta)$, is a circular Gaussian function which may be written

$$F(\theta) = (1/2\pi\theta_0^2) \exp(-\theta^2/2\theta_0^2), \quad (9)$$

where $\theta^2 = \theta_x^2 + \theta_y^2$. Integrating around a circle of radius θ we find that the fraction of incident flux which is scattered through angles between θ and $\theta + d\theta$ is

$$F(\theta) d\theta = (\theta/\theta_0^2) \exp(-\theta^2/2\theta_0^2) d\theta. \quad (10)$$

It should be noted that in deriving equations (9) and (10) no assumptions have been made about the thickness of the medium in the z direction.

(b) *Time Delays associated with Scattering*

Consider a radiation source and an observer on opposite sides of a scattering medium, their distances from the medium being xR and $(1-x)R$ respectively. As a result of geometric path differences alone (see Fig. 4) radiation scattered through an angle θ is delayed relative to unscattered radiation by a time

$$t = x(1-x)R\theta^2/2c. \quad (11)$$

This time delay may be expressed as a phase delay

$$\Phi = 2\pi\nu t = 2\pi\nu x(1-x)R\theta^2/2c. \quad (11a)$$

There will be additional components of variable phase imposed within the medium itself. However, under certain circumstances these may be neglected with no great loss of accuracy.

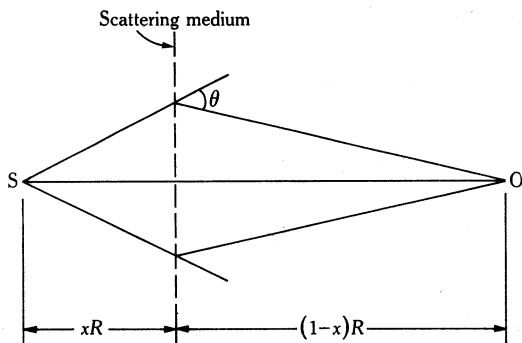


Fig. 4.—Diagram illustrating the relation between the scattering angle θ and the excess path length of the scattered radiation, from which the associated time and phase delays may be derived.

First consider a thin medium, i.e. one for which the thickness L is $\ll z_0$, where z_0 is given by $z_0 \theta_0 \approx a$ with a the scale size of a single irregularity. Such a medium merely imposes phase fluctuations on the emergent wave front, of r.m.s. magnitude ϕ , given by

$$\phi \approx \left(\sum_{k=1}^n (\delta\phi_k)^2 \right)^{\frac{1}{2}},$$

where $\delta\phi_k$ is the r.m.s. phase fluctuation imposed by the k th screen. If the distances of source and observer from the medium are both very much greater than z_0 , then for all but the very smallest values of θ , the phase delay Φ given by equation (11a) will be very much greater than ϕ (Scheuer 1968).

A thick medium, for which L is $\geq z_0$, imposes additional phase variations on the emergent wave front of approximate magnitude $\pi\nu L\theta_0^2/c$. Provided the distances of source and observer in this case are both very much greater than L , these are generally insignificant compared with Φ .

(c) *Pulsed Radiation : The Impulse Response Function*

The fraction of flux density scattered through angles between θ and $\theta+d\theta$ is given by equation (10) and the time delay associated with a given value of θ by equation (11). If the source emits a pulse of negligibly short duration we find, on

combining these two equations, that the instantaneous received flux density is proportional to $f(t, \tau)$, where $f(t, \tau)$ has the form (1) of Section III. That is, under the assumed conditions the received pulse has the form of a truncated exponential. Times are measured from the instant at which the unscattered pulse would have been received, and the scattering time

$$\begin{aligned}\tau &= x(1-x)R\theta_0^2/c \\ &= x(1-x)(R/c)(\lambda\phi/2\pi a)^2\end{aligned}\quad (12)$$

$$= x(1-x)(r_0/2\pi)^2 Rc^3 \{L(\Delta N)^2/a\} \nu^{-4} \quad (13)$$

(see equations (11), (10), (8), and (7)). We have previously referred to $f(t, \tau)$ as the impulse response function of the medium.

For a pulse of finite duration such that in the absence of scattering the instantaneous received flux density would be $s(t)$, the effect of scattering is equivalent to convolving $s(t)$ with $f(t, \tau)$, that is, the received flux density is given by

$$r(t) = \int_{-\infty}^{+\infty} s(u) f(t-u) du.$$

Assuming that $s(t) = 0$ for $t < 0$, and referring to equation (1), we derive

$$r(t) = \tau^{-1} \exp(-t/\tau) \int_0^t s(u) \exp(u/\tau) du. \quad (14)$$

Before proceeding we note that, according to our observations, ϕ , the r.m.s. variation of the phase change through the medium, is indeed very large, as initially stated in Section IV(a). As shown in Section III(a) our measured value of $\tau(300) = 9.4$ ms. This value, taken in conjunction with an upper limit of about 10^{12} cm for the irregularity scale size (Ables, Komesaroff, and Hamilton 1970) and a distance R to the pulsar of 1.5×10^{21} cm, when substituted into equation (12) yields a value for ϕ of about 6×10^4 rad at 300 MHz.

(d) Repetitive Pulses

If the source emits a succession of pulses equally spaced in time with a repetition period T , we may write $s(t) = s(t-nT)$, where n is any integer. The expression for the received flux density derived by convolving $s(t)$ with $f(t, \tau)$ is

$$r(t) = \tau^{-1} \exp(-t/\tau) \left(\frac{\exp(-T/\tau)}{1 - \exp(-T/\tau)} \int_0^T s(u) \exp(u/\tau) du + \int_0^t s(u) \exp(u/\tau) du \right), \quad (15)$$

a result somewhat more general than that derived by Cronyn (1970). It is clear that for $\tau \ll T$, equation (15) becomes identical with (14). Furthermore, it is easily shown that for the periodic waveform $r(t)$ given by equation (15),

$$\int_0^T r(t) dt = \int_0^T s(t) dt,$$

corresponding to the obvious physical fact that scattering involves no loss of energy. However, $r(t)$ does not decrease to zero between pulses; its minimum value is $r(T)$.

Therefore a component $Tr(T)$ of the pulsed emission is converted to steady emission by the scattering process. The fraction of energy which remains pulsed after scattering is

$$J_p = 1 - Tr(T) / \left(\int_0^T s(t) dt \right). \quad (16)$$

For finite values of T/τ

$$J_p \lesssim 1 - \frac{(T/\tau) \exp(-T/\tau)}{\{1 - \exp(-T/\tau)\}},$$

so that we have $J_p \rightarrow T/2\tau$ for $\tau \gg T$. As $T/2\tau$ decreases through unity with decreasing frequency, J_p decreases rapidly.

(e) Effect on Polarization

We see that scattering involves the incoherent addition of radiation components emitted at different times during the pulse. The polarization of these components is not affected by the scattering, provided the scattering angle θ is $\ll 1$, and provided magnetic fields in the scattering region may be neglected.

It follows that the time-dependent intensity and polarization of the pulse after scattering may be computed by convolving each of the time-dependent Stokes parameters of the unscattered pulse with the impulse response function of the medium, which for the case we have considered is the truncated exponential $f(t, \tau)$.

V. EFFECTS OF SCATTERING IN INTERSTELLAR MEDIUM AND NEAR PULSAR

According to Brandt *et al.* (1971), PSR 0833-45, observed to lie in the direction of the Gum nebula, is actually situated near the centre of that nebula, which is the largest known ionized hydrogen region in the Galaxy. Considering the very short period of the pulsar, it is therefore not surprising that its pulses are markedly affected by scattering.

From $H\alpha$ emission measures made by Gum (1952), Brandt *et al.* (1971) estimate typical r.m.s. electron densities of about 1.3 cm^{-3} , but this presumably refers to aggregates of very much larger linear dimensions than the "fine structure" producing the scattering. Ables, Komesaroff, and Hamilton (1970) have set an upper limit of between 10^{12} and 10^{13} cm on the scale of this fine structure. Even if the strong scattering medium does not extend over more than 10 pc (or 2% of the distance to the pulsar), the r.m.s. electron density fluctuations required to explain the scattering do not exceed about 0.6 cm^{-3} and may be less; this represents only a weak density modulation within a larger aggregate. The required number of such small-scale irregularities along the line of sight is between 3×10^6 and 3×10^7 .

The simple scattering model leading to a truncated exponential impulse response function provides a reasonable explanation of the observed low-frequency pulse characteristics. This contrasts with results obtained by Rankin *et al.* (1970) from observations of NP 0532. They found that for this pulsar, as observed prior to 1970, the impulse response function was of the form

$$\begin{aligned} g(t, \tau) &= (t/\tau^2) \exp(-t/\tau) & \text{for } t \geq 0, \\ &= 0 & t < 0. \end{aligned}$$

They point out that $g(t, \tau)$ is the convolution of two truncated exponentials $f(t, \tau_1)$ and $f(t, \tau_2)$ for the limiting case in which $\tau_1 = \tau_2$. However, in a more recent paper Counselman and Rankin (1971) have shown that there were large changes in the form of the function during 1970, and that all the observations can be explained on the assumption that τ_1 remained constant, but that τ_2 decreased to zero during 1970. Thus at the end of 1970 the impulse response function derived by them was also a truncated exponential. The constancy of τ_1 suggests that it is to be associated with scattering from the general interstellar medium, and the relatively fast variability of τ_2 suggests an effect originating much closer to the pulsar. Indeed Counselman and Rankin mention that significant scattering may take place in the Crab nebula.

Now, Komesaroff (1971) has pointed out that many features of the NP0532 precursor pulse may be explained in terms of scattering of the main pulsar radiation from a ring of material lying close to the velocity-of-light cylinder. As indicated in Section III, there are suggestions of effects similar to the NP0532 precursor observed in the case of PSR 0833—45. If the explanation of the precursor is correct, it would allow us to discriminate between different models of the pulsar emission process.

VI. RADIATION MECHANISMS

According to most explanations, pulsar radiation originates close to the surface of the central neutron star, or at least not much further than the velocity-of-light radius. Lerche (1970*a*, 1970*b*, 1970*c*), on the other hand, has advanced the interesting suggestion that the radiation is produced at a boundary between the interstellar medium and a cavity surrounding the star. The radius of this boundary is very much greater than the velocity-of-light radius.

Clearly, if the precursor is to be explained in terms of scattering from close to the velocity-of-light cylinder, the radiation must originate from a source closer to the stellar surface. Thus it would be possible to discriminate between pulsar models if definite evidence of "close in" scattering could be found. Low-frequency measurements of both pulsed and continuous emission might provide such evidence.

One aspect of these and other observations should be stressed and must be taken into account by any theory which has the radio emission generated close to the stellar surface. The present results together with those of Ekers *et al.* (1969) and Radhakrishnan and Cooke (1969) demonstrate that the instantaneous position angle of the linear polarization is invariant over a frequency range of more than 7:1, when allowance has been made for interstellar Faraday rotation and scattering. The results of Morris, Schwarz, and Cooke (1970), Schwarz and Morris (1971), and Manchester (1971*a*, 1971*b*) indicate frequency invariance of position angle for most other pulsars.

Since a rotating neutron star is believed to possess a dense magnetosphere (Goldreich and Julian 1969) and a very intense magnetic field, these would be expected to modify the emergent polarization even if the latter were frequency-invariant at the point of generation. One possible resolution of this apparent impasse has been suggested by Komesaroff, Ables, and Hamilton (1971), based on a model due to Sturrock (1971).

VII. ACKNOWLEDGMENTS

The authors are indebted to Dr. B. J. Robinson and Dr. J. A. Roberts for considerable help in the preparation of this manuscript. They also thank Mrs. R. Otrupcek for her assistance with computations.

VIII. REFERENCES

- ABLES, J. G., KOMESAROFF, M. M., and HAMILTON, P. A. (1970).—*Astrophys. Lett.* **6**, 129.
BRAMLEY, E. N. (1954).—*Proc. R. Soc. A* **225**, 515.
BRANDT, J. C., STECHER, T. P., CRAWFORD, D. L., and MARAN, S. P. (1971).—*Astrophys. J.* **163**, L99.
CAMPBELL, D. B., HEILES, C., and RANKIN, J. M. (1970).—*Nature* **225**, 527.
COUNSELMAN, C. C., and RANKIN, J. M. (1971).—*Astrophys. J.* **166**, 513.
CRONYN, W. M. (1970).—*Science, N.Y.* **168**, 1453.
EKERS, R. D., LEQUEUX, J., MOFFET, A. T., and SEIELSTAD, G. A. (1969).—*Astrophys. J.* **156**, L21.
FEJER, J. A. (1953).—*Proc. R. Soc. A* **220**, 455.
GOLDREICH, P., and JULIAN, W. H. (1969).—*Astrophys. J.* **157**, 869.
GUM, C. S. (1952).—*Observatory* **72**, 151.
HEWISH, A. (1951).—*Proc. R. Soc. A* **209**, 81.
HIGGINS, C. S., KOMESAROFF, M. M., and SLEE, O. B. (1971).—*Astrophys. Lett.* **9**, 75.
KOMESAROFF, M. M. (1971).—*Astrophys. Lett.* **9**, 195.
KOMESAROFF, M. M., ABLES, J. G., and HAMILTON, P. A. (1971).—*Astrophys. Lett.* **9**, 101.
KOMESAROFF, M. M., HAMILTON, P. A., and ABLES, J. G. (1971).—*Proc. IAU Symp. No. 46 on Crab Nebula.* (Eds. R. D. Davies and F. G. Smith.) p. 217. (Reidel: Dordrecht, Holland.)
LERCHE, I. (1970a).—*Astrophys. J.* **159**, 229.
LERCHE, I. (1970b).—*Astrophys. J.* **160**, 1003.
LERCHE, I. (1970c).—*Astrophys. J.* **162**, 153.
McCULLOCH, P. M., HAMILTON, P. A., ABLES, J. G., and KOMESAROFF, M. M. (1972).—*Astrophys. Lett.* **10**, 163.
MANCHESTER, R. N. (1971a).—*Astrophys. J. Suppl. Ser.* **199**, 283.
MANCHESTER, R. N. (1971b).—*Nature Phys. Sci.* **231**, 189.
MORRIS, D., SCHWARZ, U. J., and COOKE, D. J. (1970).—*Astrophys. Lett.* **5**, 181.
PAPOULIS, A. (1965).—"Probability, Random Variables, and Stochastic Processes." p. 337. (McGraw-Hill: New York.)
RADHAKRISHNAN, V., and COOKE, D. J. (1969).—*Astrophys. Lett.* **3**, 225.
RADHAKRISHNAN, V., COOKE, D. J., KOMESAROFF, M. M., and MORRIS, D. (1969).—*Nature* **221**, 443.
RANKIN, J. M., COMELLA, J. M., CRAFT, H. D., RICHARDS, D. W., CAMPBELL, D. B., and COUNSELMAN, C. C. (1970).—*Astrophys. J.* **162**, 707.
RANKIN, J. M., HEILES, C., and COMELLA, J. M. (1971).—*Astrophys. J.* **163**, L95.
RATCLIFFE, J. A. (1956).—*Rep. Prog. Phys.* **19**, 188.
SCHEUER, P. A. G. (1968).—*Nature* **218**, 920.
SCHWARZ, U. J., and MORRIS, D. (1971).—*Astrophys. Lett.* **7**, 185.
STURROCK, P. A. (1971).—*Astrophys. J.* **164**, 529.

